

Slow Dynamics of Nonequilibrium Density Fluctuations in Concentrated Hard-Sphere Suspensions¹

M. Tokuyama,^{2,3} Y. Enomoto,⁴ and I. Oppenheim⁵

The coupled diffusion equations recently proposed for concentrated hard-sphere suspensions of interacting Brownian particles, the nonlinear deterministic diffusion equation with the self-diffusion coefficient $D_S(\Phi(\mathbf{x}, t))$ for the average local volume fraction $\Phi(\mathbf{x}, t)$, and the linear stochastic diffusion equation with $D_S(\Phi(\mathbf{x}, t))$ for the density fluctuations $\delta n(\mathbf{x}, t)$ are numerically solved under a spatially inhomogeneous, nonequilibrium initial state. Thus, in a supercooled region where $\phi_p \leq \phi < \phi_g$, the slow evolution of the cluster-like glassy domains with $\phi(\mathbf{x}, t) \geq \phi_g$ and the slow relaxation of the nonequilibrium density fluctuations are shown to be caused by the dynamic singularity of the self-diffusion coefficient, $D_S(\Phi(\mathbf{x}, t)) \sim (1 - \Phi(\mathbf{x}, t)/\phi_g)^2$, where ϕ is a particle volume fraction, $\phi_g = (4/3)^3 / (7 \ln 3 - 8 \ln 2 + 2)$ is the colloidal glass transition volume fraction, and ϕ_p is the crossover volume fraction.

KEY WORDS: crossover volume fraction; dynamic singularity; irregularly shaped glassy domain; slow dynamics; spatial inhomogeneities; supercooled colloidal fluid.

1. INTRODUCTION

In this paper we study the nonequilibrium effect on the slow dynamics of concentrated hard-sphere suspensions near ϕ_g . Many attempts to understand

¹ Paper presented at the Thirteenth Symposium on Thermophysical Properties, June 22–27, 1997, Boulder, Colorado, U.S.A.

² Statistical Physics Division, Tohwa Institute for Science, Tohwa University, Fukuoka 815, Japan.

³ To whom correspondence should be addressed.

⁴ Graduate School of Engineering, Nagoya Institute of Technology, Nagoya 466, Japan.

⁵ Department of Chemistry, Massachusetts Institute of Technology, Cambridge, Massachusetts 02139, U.S.A.

the dynamics of colloidal suspensions approaching the glass transition have been made by employing the mode-coupling theory (MCT) [1, 2] for the dynamics of supercooled fluids. Hence, much of the recent experimental studies [3, 4] of slow relaxation in colloidal fluids has been designed around the predictions of MCT. Recently, the model equations described below have been shown asymptotically [5], analytically [6], and numerically [7] to exhibit a number of the characteristic features of slow relaxation of a colloidal fluid [8]. These include a divergence of relaxation times at ϕ_g and a two-step relaxation of the self-intermediate scattering function with time. Although the results similar to those obtained by MCT have been found, the basic standpoints in two theories are quite different. First, MCT has been applied to equilibrium systems where the average number density $n(\mathbf{x}, t)$ becomes constant n_0 in space and time, that is, $\Phi(\mathbf{x}, t) = (4\pi a_0^3/3) n(\mathbf{x}, t)$ reaches the equilibrium volume fraction $\phi = 4\pi a_0^3 n_0/3$, where a_0 is the particle radius. On the other hand, the present theory deals with a spatially inhomogeneous, nonequilibrium system, which obeys the nonlinear deterministic diffusion equation for $\Phi(\mathbf{x}, t)$. This is because most experimental measurements near ϕ_g are done in quenched metastable fluid states where equilibration of a colloidal fluid is nearly impossible on laboratory time scales. Second, MCT assumes that the density fluctuations $\delta(\mathbf{x}, t)$ around n_0 obey the nonlinear stochastic equations. On the other hand, the present theory starts with the linear stochastic diffusion equation for the density fluctuations $\delta n(\mathbf{x}, t)$ around $n(\mathbf{x}, t)$. This is because the density fluctuations would be small compared to the causal part $n(\mathbf{x}, t)$ since the glass transition seems not to be a critical phenomenon. In fact, there is no correlation length diverging at the glass transition point. Hence, the glass transition seems to be dynamic in origin in contrast to critical phenomena. Finally, MCT contains two parameters, the volume fraction ϕ and a microscopic time scale t_0 , which is treated as a free fit parameter. On the other hand, the present theory contains two parameters, ϕ , and the initial number density $n(\mathbf{x}, 0)$, both of which are fixed by experiment. The main results reported here are (i) the existence of an crossover volume fraction ϕ_β , over which the slow dynamical behavior appears, (ii) three characteristic stages in the supercooled region $\phi_\beta \leq \phi < \phi_g$, and (iii) slow dynamics of long-lived, irregularly shaped glassy domains with $\Phi(\mathbf{x}, t) \geq \phi_g$ in the supercooled region.

2. THE MODEL EQUATIONS

The causal motion of colloidal suspensions is described by the local volume fraction $\Phi(\mathbf{x}, t)$. On the other hand, the dynamics of density fluctuations can be measured by dynamic light scattering through the intermediate

scattering function [9], which is given by the Fourier transform, $F(\mathbf{k}, t)$, of the autocorrelation function of the density fluctuations $F(\mathbf{x}, t) = \langle \delta n(\mathbf{x}, t) \delta n(\mathbf{0}, 0) \rangle / N$, where the angular brackets denote the average over the canonical ensemble and N is the total number of particles. For scattering vectors much larger than the maximum position k_m of the structure factor $S(\mathbf{k}) = F(\mathbf{k}, 0)$, the scattering function $F(\mathbf{k}, t)$ reduces to the self-intermediate scattering function $F_S(\mathbf{k}, t)$, where $F_S(\mathbf{k}, 0) = S(\mathbf{k}) = 1$. Hence we start with the following coupled diffusion equations already described elsewhere [5]:

$$\frac{\partial}{\partial t} \Phi(\mathbf{x}, t) = \nabla \cdot [D_S(\Phi(\mathbf{x}, t)) \nabla \Phi(\mathbf{x}, t)] \quad (1)$$

$$\frac{\partial}{\partial t} F_S(\mathbf{k}, t) = -k^2 \sum_{\mathbf{q}} D_S(\mathbf{k} - \mathbf{q}, t) F_S(\mathbf{q}, t) \quad (2)$$

with the Fourier transform, $D_S(\mathbf{k}, t)$, of the self-diffusion coefficient

$$D_S(\Phi(\mathbf{x}, t)) = \frac{D_S^S(\phi)(1 - 9\Phi(\mathbf{x}, t)/32)}{[1 + (\Phi(\mathbf{x}, t) D_S^S(\phi)/\phi_g D_0)(1 - \Phi(\mathbf{x}, t)/\phi_g)^{-2}] \quad (3)$$

and the conservation law $(1/V) \int d\mathbf{x} \Phi(\mathbf{x}, t) = \phi$, where D_0 is the single-particle diffusion coefficient, $D_S^S(\phi)$ is the short-time self-diffusion coefficient (see Ref. 10 for details), and V is the total volume of the system. Here the factor $(9/32)$ in the numerator of Eq. (3) results from the coupling between the direct and the short-range hydrodynamic interactions among particles, while the second singular term in the denominator originates from the many-body correlations of long-range hydrodynamic interactions between particles [10]. Equation (1) describes a nonequilibrium transitional behavior from a spatially inhomogeneous initial state with $\Phi(\mathbf{x}, 0)$ to an equilibrium state with $\Phi(\mathbf{x}, \infty) = \phi$, while Eq. (2) describes a linear relaxation of $F_S(\mathbf{k}, t)$ on the nonequilibrium state $\Phi(\mathbf{x}, t)$. For short times $t \ll t_\gamma = 2\pi/(k^2 D_S^S)$, $D_S(\Phi)$ reduces to $D_S^S(\phi)$ since the direct interactions and the correlations are negligible, while for long times $t \gg t_\alpha = 2\pi/(k^2 D_S^L)$, it reduces to the long-time self-diffusion coefficient $D_S^L(\phi) = D_S(\Phi)$ [10]. In Fig. 1 we plot the theoretical and experimental results for the normalized self-diffusion coefficient, D_S/D_0 , as a function of the volume fraction ϕ for short and long times. Good agreement is indeed seen between the theoretical results and the experimental data. Thus, there exists a crossover from the short-time process described by D_S^S to the long-time process described by D_S^L for intermediate times, where the dynamic singularity, $D_S(\Phi) \sim (1 - \Phi(\mathbf{x}, t)/\phi_g)^2$, becomes important.

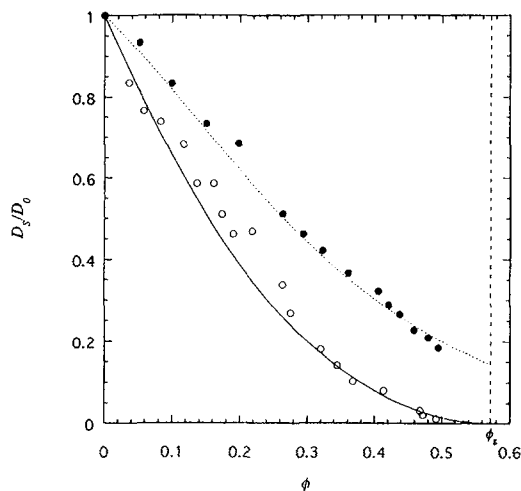


Fig. 1. Normalized self-diffusion coefficient, D_s/D_0 , as a function of volume fraction ϕ . The dotted line indicates the short-time self diffusion coefficient D_s^S , and the solid line the long-time self-diffusion coefficient D_s^L . Also shown are the data from Ref. 12 (●) and Ref. 13 (○).

3. RESULTS

In order to solve the coupled diffusion Eqs. (1) and (2) self-consistently, we first fix the values of the two parameters as the initial conditions, the particle volume fraction ϕ and the initial local volume fraction $\Phi(\mathbf{x}, 0)$. To integrate those equations, we employ the forward Euler difference scheme with the time step $0.01a_0^2/D_0$ and the lattice spacing $0.2a_0$ in the volume $(128a_0)^3$ of the three-dimensional simulation system with periodic boundary conditions. In order to distinguish the initial states from each other qualitatively, it is convenient to introduce a state parameter z_0 by [7]

$$z_0 = 1 - (1/V) \int d\mathbf{x} |1 - \Phi(\mathbf{x}, 0)/\phi| \quad (4)$$

This parameter measures how close the initial state of the system is to the equilibrium state, where $0 \leq z_0 < 1$ for a nonequilibrium initial state, and $z_0 = 1$ for an equilibrium initial state. The initial value $\Phi(\mathbf{x}, 0)$ is chosen at each position \mathbf{x} from a random number with a Gaussian distribution,

which is characterized by a mean value 1 and a standard deviation s , where s is adjusted so as to satisfy Eq. (4) for a given value z_0 .

As shown in Refs. 5–7, there are, in general, three characteristic stages in the colloidal fluid for $0 < \phi < \phi_g$. The first is an early stage [E] for $t_B \ll t \ll t_y$, where t_B is the Brownian relaxation time. The spatial inhomogeneities are described by $\Phi(\mathbf{x}, t) \simeq \exp(-tD_S^S \nabla^2) \Phi(\mathbf{x}, 0)$, and the density fluctuations obey the short-time exponential decay $F_S^S(\mathbf{k}, t) = \exp(-k^2 D_S^S t)$, where the system is occupied by the colloidal fluid with D_S^S . The second is an intermediate stage [I] for $t_y \ll t \ll t_x$, where the dynamical behavior is complicated because of the singularity of $D_S(\Phi)$. The last is a late stage [L] for $t \geq t_x$. $\Phi(\mathbf{x}, t)$ becomes homogeneous in space and time, reaching ϕ , and $F_S(\mathbf{k}, t)$ obeys the long-time exponential decay $F_S^L(\mathbf{k}, t) = \exp(-k^2 D_S^L t)$, where the system is occupied by the colloidal fluid with D_S^L .

In Fig. 2 we show the time evolution of $F_S(\mathbf{k}, t)$ at $z_0 = 0.5$ and 0.8 for $\phi = 0.543$, $\phi_\beta(z_0, ka_0)$, and 0.571 , where ϕ_β is the crossover volume fraction discussed below. Below ϕ_β , the scattering function $F_S(\mathbf{k}, t)$ decays quickly to zero, while above ϕ_β , the shape of $F_S(\mathbf{k}, t)$ becomes very sensitive to the value of ϕ , forming a shoulder, which becomes at ϕ_g a plateau with the height $f_k^c(z_0) = \lim_{t \rightarrow \infty} F_S(\mathbf{k}, t; \phi = \phi_g)$ [5–7]. Thus, the dynamical behavior of the so-called supercooled region ($\phi_\beta \leq \phi < \phi_g$) in stage [I] is quite different from that of the normal region ($0 < \phi < \phi_\beta$).

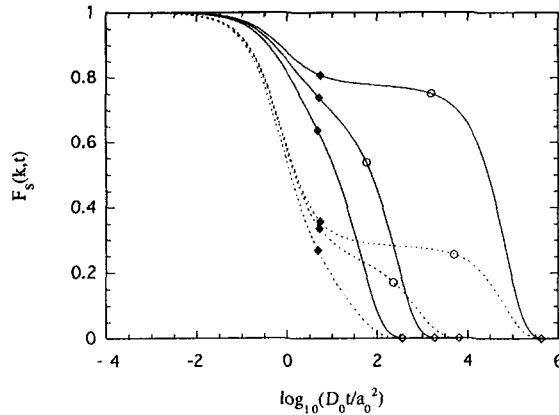


Fig. 2. Self-intermediate scattering function $F_S(k, t)$ versus dimensionless time $D_0 t / a_0^2$ for different volume fractions (from left to right): 0.543, $\phi_\beta(z_0, ka_0)$ and 0.571 at $z_0 = 0.8$ (solid lines) and 0.5 (dotted lines), where $\phi_\beta(0.8, 3.42) = 0.5591$ and $\phi_\beta(0.5, 3.42) = 0.5648$. The symbols indicate the time scales: t_y (\blacklozenge), t_β (\circ), and t_x (\diamond).

In order to see the crossover behavior in stage [I] more clearly, we next calculate the logarithmic derivatives given by $\varphi = \partial \log |f_k^c - F_S(\mathbf{k}, t)| / \partial \log t$ and $\varphi' = \partial \varphi / \partial \log t$ [5–7]. Then, $\varphi' = 0$ gives two time roots, $t_{b_0}(\phi, z_0, k)$ and $t_b(\phi, z_0, k)$, which reveal two fairly flat regions: $\varphi = b_0(\phi, z_0, k)$ at $t = t_{b_0}$, where $t_\gamma \ll t_{b_0} \ll t_\beta$, and $\varphi = b(\phi, z_0, k)$ at $t = t_b$, where $t_\beta \ll t_b \ll t_\alpha$. Here $t_\beta = 2\pi / (k^2 (D_S^S D_S^L)^{1/2})$ indicates a crossover time and becomes singular as $t_\beta \sim (1 - \phi/\phi_g)^{-1}$ near ϕ_g since $t_\alpha \sim (1 - \phi/\phi_g)^{-2}$ [6]. Then, the crossover volume fraction $\phi_\beta(z_0, k)$ is determined by the equal root $t_{b_0}(\phi_\beta, z_0, k) = t_b(\phi_\beta, z_0, k)$, or $b_0(\phi_\beta, z_0, k) = b(\phi_\beta, z_0, k)$ at fixed values of z_0 and k [11]. With increasing volume fraction at a fixed z_0 , we thus observe a progression from colloidal fluid ($0 < \phi < \phi_\beta$), to supercooled colloidal fluid ($\phi_\beta \leq \phi < \phi_g$), to glass ($\phi \geq \phi_g$) (see Fig. 3). In the supercooled region, therefore, $F_S(\mathbf{k}, t)$ obeys two kinds of power-law decays with exponents b_0 and b around t_β [5–7]. Thus, the intermediate stage further separates into two stages. One is a formation stage [F] for $t_\gamma \ll t \ll t_\beta$. As shown in Fig. 4, the glassy regions where $\Phi(\mathbf{x}, t)$ is larger than ϕ_g form finite-sized, long-lived, irregularly shaped domains. Because of these domains, the smoothing process of the spatial inhomogeneities to the uniform state is slowing down, leading to a structural arrest. Hence, the density fluctuations also undergo a slow relaxation and obey the power-law decay,

$$F_S^F(\mathbf{k}, t) = f_k^c(z_0) - A_k(z_0)(t/t_\beta)^{b_0} \quad (5)$$

where $A_k = [f_k^c - F_S(\mathbf{k}, t_{b_0})](t_\beta/t_{b_0})^{b_0}$. This power-law decay continues up to the crossover time t_β . For $t \geq t_\beta$, the shrinkage stage [Sh] starts, where

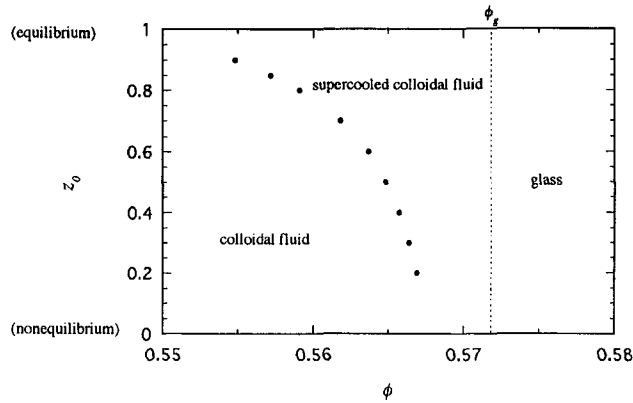


Fig. 3. Schematic phase diagram in the ϕ - z_0 plane for hard-sphere suspensions. The filled circles indicate the crossover volume fraction ϕ_β , and the dotted line the glass transition volume fraction ϕ_g .

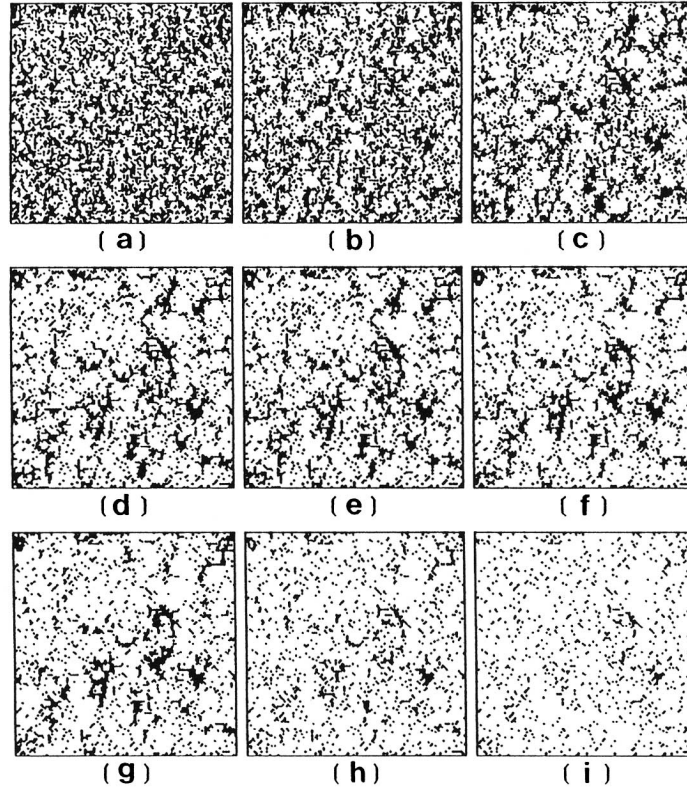


Fig. 4. Typical configurations, projected onto a plane, of pattern-evolution processes at $\phi = 0.571$ and $z_0 = 0.8$ in the supercooled region $\phi_\beta \leq \phi < \phi_B$ for dimensionless times (a) 1, (b) $6.35(t_x)$, (c) 10^2 , (d) 10^3 , (e) $1279(t_x)$, (f) 10^4 , (g) 10^5 , (h) $4.4 \times 10^5(t_x)$, and (i) 10^6 . The system size is $(128a_0)^2$, and the glassy regions are colored black.

the glassy domains start to shrink (see Fig. 4). Since the glassy domains disappear very slowly, the relaxation of the density fluctuations also becomes slow and obeys the so-called von Schweidler decay,

$$F_S^{\text{Sh}}(\mathbf{k}, t) = f_k^c(z_0) - B_k(z_0)(t/t_x)^b \quad (6)$$

where $B_k = [f_k^c - F_S(\mathbf{k}, t_b)](t_x/t_b)^b$. The power-law decay continues up to the long time t_x , over which the glassy domains disappear. Figure 5 shows schematically the characteristic stages in the supercooled region. On the other hand, in stage [I] of the normal region there is neither a formation of finite-sized glassy domains nor a power-law decay. Hence, the spatial inhomogeneities become smooth monotonical, obeying Eq. (1), while the

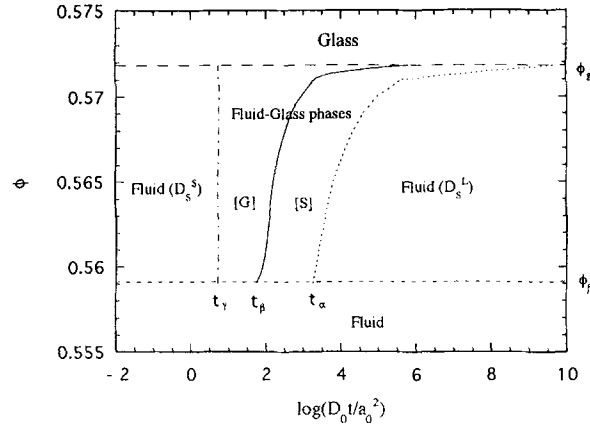


Fig. 5. Characteristic stages in the supercooled region $\phi_\beta \leq \phi < \phi_g$ at $z_0 = 0.8$ and $ka_0 = 3.42$. The dot-dashed line indicates the characteristic time t_γ , the solid line t_β , and the dotted line t_α .

relaxation gradually changes from the short-time exponential decay $F_S^S(\mathbf{k}, t)$ to the long-time exponential decay $F_S^L(\mathbf{k}, t)$.

4. CONCLUSION

In conclusion, we have shown that there exists the supercooled region ($\phi_\beta \leq \phi < \phi_g$), in which the fluid and irregularly shaped glass phases coexist on the time scale of order $t_\beta(\phi, k)$ and the stow dynamics occur. We emphasize that these originate from the dynamic singularity of $D_S(\Phi)$. As shown in Fig. 3, the supercooled region becomes wide as z_0 increases, and ϕ_β is expected to coincide with the melting volume fraction $\phi_m = 0.545$ in equilibrium ($z_0 = 1$). Finally, we should refer to how the present theory relates to experiments. By fitting the theoretical plateau height $f_k^c(z_0)$ with experimental results at a given value of \mathbf{k} , one can calculate the state parameter z_0 theoretically. Hence, one can guess how far from equilibrium the experimental system is initially. Once the value of z_0 is found, one can thus analyze experimental results in terms of the present theory for different volume fractions. This will be discussed elsewhere.

ACKNOWLEDGMENT

This work was supported by the Tohwa Institute for Science, Tohwa University.

REFERENCES

1. W. Götze and L. Sjögren, *Phys. Rev. A* **43**:5442 (1991).
2. U. Bengtzelius, W. Götze, and A. Sjölander, *J. Phys. C* **17**:5915 (1984).
3. P. N. Pusey and W. van Meegen, *Nature* **320**:340(1986).
4. W. van Meegen and S. M. Underwood, *Phys. Rev. E* **49**:4206 (1994).
5. M. Tokuyama, *Physica A* **229**:36 (1996).
6. M. Tokuyama, *Phys. Rev. E* **54**:R1062 (1996).
7. M. Tokuyama, Y. Enomoto, and I. Oppenheim, *Phys. Rev. E* **55**:R29 (1997).
8. P. N. Pusey, in *Liquids, Freezing and the Glass Transition*, D. Levesque, J. P. Hansen, and J. Zinn-Justin, eds. (Elsevier, Amsterdam, 1991).
9. B. J. Berne and R. Pecora, *Dynamic Light Scattering* (Wiley, New York, 1976).
10. M. Tokuyama and I. Oppenheim, *Physica A* **216**:85 (1995).
11. M. Tokuyama, *Prog. Theor. Phys. Suppl.* **126**:43 (1997).
12. P. N. Segrè, O. P. Behrend, and P. N. Pusey, *Phys. Rev. E* **52**:5070 (1995).
13. W. Van Meegen and S. M. Underwood, *J. Chem. Phys.* **91**:552 (1989).